BNL-104728-2014-TECH

AGS/AD/Tech Note No. 312;BNL-104728-2014-IR

SUBHARMONIC RIPPLE REDUCTION LIMIT IN MULTIPHASE RECTIFIERS

S. Y. Zhang

January 1989

Collider Accelerator Department

Brookhaven National Laboratory

U.S. Department of Energy

USDOE Office of Science (SC)

DISCLAIMER

Accelerator Division
Alternating Gradient Synchrotron Department
BROOKHAVEN NATIONAL LABORATORY
Associated Universities, Inc.
Upton, New York 11973

Accelerator Division
Technical Note

AGS/AD/Tech. Note No. 312

SUBHARMONIC RIPPLE REDUCTION LIMIT IN MULTIPHASE RECTIFIERS

S.Y. Zhang and A.V. Soukas

January 12, 1989

I. Introduction

In a multiphase rectifier system, the SCR firing time is controlled by the triggering circuits according to the requirement of the rectifier DC output voltage. As far as the subharmonic ripple is concerned, if the cause of the ripple appears due to the inadequacies of the firing circuits, then this ripple can be completely corrected. On the other hand, if the ripple is caused by the transformer imbalance, power line imbalance, commutation imbalance, etc, then the waveforms of the individual phases supplied to the SCR bridges would be imbalanced, and it is observed that there is a limit for the reduction of this type ripple. If further ripple reduction is necessary, then the only means is to fix the power supply waveform imbalance. Since such a problem is often encountered in practice, it is of interest to examine it further.

In this note, we study the problem by using an analytical means. The ripple to be studied is the one that often catches attention, i.e., the 360Hz ripple in a 12 phase rectifier. It is well known that the control of the 360Hz ripple is difficult. The reason is multifold. First, only 2 sampling points for each cycle of the 360Hz ripple in a 12 phase rectifier can be controlled. According to Sampling Theory, 360Hz is the highest frequency component that can be recovered from the 12 phase sampling. Secondly, because of the

transformer structures chosen for a 12 phase rectifier system, the most significant power supply waveform imbalance is 360Hz, therefore the limit for the 360Hz ripple component is remarkably higher than the others, and also it is difficult to reduce.

II. Ripple Reduction Limit Analysis

1. Transformer amplitude imbalance

Consider the rectified waveform shown in Fig.1, where the sine waveforms are with the fundamental frequency ω_0. Every subsequent sine waveform is delayed by τ second. Let the first waveform be sampled by the solid vertical line at τ_0, and the second at $\tau_0+\tau$, and so on. Since such a sampling is equally spaced in time, we call it uniform sampling. Let the control be such defined that the first and second sampling times will move by amounts denoted by α and β in the directions shown in Fig.1. Let the first waveform have the amplitude 1(unity) and the second the k. If we use the step function $u(t)$, then the waveform in Fig.1 from the first sampling to the third sampling can be written as

$$\begin{aligned} f(t) &= [u(t)-u(t-\tau-\alpha-\beta)]Sin\,\omega_0(t+\tau_0-\alpha) \\ &+ k[u(t-\tau-\alpha-\beta)-u(t-2\tau)]Sin\,\omega_0(t+\tau_0-\tau-\alpha) \end{aligned} \tag{1}$$

The Fourier transform of the function $f(t)$ can be written as

$$\begin{aligned} F(j\omega) = \frac{1}{\omega_0^2-\omega^2}\{&\omega_0 Cos\,\omega_0(\tau_0-\alpha) + j\,\omega Sin\,\omega_0(\tau_0-\alpha) \\ &- \omega_0 Cos\,\omega(\tau+\alpha+\beta)Cos\,\omega_0(\tau+\tau_0+\beta) + j\,\omega_0 Sin\,\omega(\tau+\alpha+\beta)Cos\,\omega_0(\tau+\tau_0+\beta) \\ &- j\,\omega Cos\,\omega(\tau+\alpha+\beta)Sin\,\omega_0(\tau+\tau_0+\beta) - \omega Sin\,\omega(\tau+\alpha+\beta)Sin\,\omega_0(\tau+\tau_0+\beta) \\ &+ k(\omega_0 Cos\,\omega(\tau+\alpha+\beta)Cos\,\omega_0(\tau_0+\beta) - j\,\omega_0 Sin\,\omega(\tau+\alpha+\beta)Cos\,\omega_0(\tau_0+\beta)) \\ &+ k(j\,\omega Cos\,\omega(\tau+\alpha+\beta)Sin\,\omega_0(\tau_0+\beta) + \omega Sin\,\omega(\tau+\alpha+\beta)Sin\,\omega_0(\tau_0+\beta)) \\ &+ k(-\omega_0 Cos\,2\omega\tau Cos\,\omega_0(\tau+\tau_0-\alpha) + j\,\omega_0 Sin\,2\omega\tau Cos\,\omega_0(\tau+\tau_0-\alpha)) \\ &+ k(-j\,\omega Cos\,2\omega\tau Sin\,\omega_0(\tau+\tau_0-\alpha) - \omega Sin\,2\omega\tau Sin\,\omega_0(\tau+\tau_0-\alpha))\} \end{aligned} \tag{2}$$

See the Appendix for details of the derivation.

For a 12 phase rectifier, we may let ω_0=120π, and τ=1.3889ms. Note that the

waveform function and the Fourier transform in (1) and (2) only represent two 720Hz sampling, or one 360Hz sampling period segment shown in Fig.1. However, if we are only interested in the DC and 360Hz components, the spectrum analysis resulting from (2) is proportional to the generic case, i.e., where waveform (1) is expanded in both directions on the time axis periodically. This fact is verified as follows. We use the time shift property of Fourier transforms, see (A-6) in the appendix, and the linearity for the superposition. Then we can write the generic waveform as

$$f(t) = \sum_{i=-\infty}^{\infty} \{[u(t-2\tau i)-u((t-2\tau i)-\tau-\alpha-\beta)]Sin\,\omega_0((t-2\tau i)+\tau_0-\alpha) + k[u((t-2\tau i)-\tau-\alpha-\beta)-u((t-2\tau i)-2\tau)]Sin\,\omega_0((t-2\tau i)+\tau_0-\tau-\alpha)\} \quad (3)$$

where i is integer. Thus, we have the spectrum for the generic waveform as

$$\sum_{i=-\infty}^{\infty} e^{j2\omega\tau i}F(j\omega) = \sum_{i=-\infty}^{\infty} (Cos2\omega\tau i + jSin2\omega\tau i)F(j\omega) \quad (4)$$

where $F(j\omega)$ is from (2). Noting that under the condition of τ=1.3889ms at either ω=0 or ω=720π we have

$$2\omega\tau i = 2n\pi$$

for all i, where n is an integer. Therefore, the equation (4) can always be written as

$$\sum_{i=-\infty}^{\infty} e^{j2\omega\tau i}F(j\omega) = \sum_{n=-\infty}^{\infty} Cos2n\pi F(j\omega), \quad \omega = 0,\ 720\pi \quad (5)$$

which shows that the spectrum (2) of the waveform (1) is proportional to the spectrum of the generic waveform, and therefore can be used in the analysis. Note that this fact is also valid for 720Hz ripple and all the harmonics.

In Fig.2a, we show the 360Hz component in the spectrum $(\omega_0^2-\omega^2)F(j\omega)$, with the sampling control of α and β is scanning from -0.69ms to 0.69ms synchronously, marked on the x-axis. The quantities α and β move by equal amounts in the directions shown in Fig.1, i.e., α leads and β lags. We note that such a firing control is a close simulation to the ripple correction by using a 360Hz sine waveform with different amplitude and phase.

The curves from the bottom to the top are for the different amounts of imbalance of k=1+ϵ, with ϵ= 0, 0.01, 0.02, 0.03, 0.04, 0.05, respectively. It shows that if the waveform is balanced(ϵ=0), then the uniform firing scheme produces no 360Hz ripple. Any drift from these balanced firing points($\alpha = \beta \neq 0$) causes an increase of the ripple. On the other hand, if the waveform is not balanced($\epsilon \neq 0$), then a value of zero for the 360Hz ripple can never be reached. The more the imbalance, the higher the ripple reduction limit. In Fig.2b, we let the DC level be 0db, and then plot the curves in a logarithmic magnitude scale for the same situation. We may read that if the waveform imbalance is 5%, then the minimum 360Hz ripple with respect to the DC level is about -37db. For smaller amounts of imbalance, lower 360Hz ripple limits can be attained. Fig.2 is plotted for a rectifier system where the phase back angle is 7.5 degrees, i.e., τ_0=4.1667ms. If the phase back angle moves to 39.9 degrees, i.e., τ_0=5.6667ms, then the curves are as replotted in Fig.3. We can observe in this case that while the average ripple is increased, the limit of the reduction is lowered. Fig.3c shows a blown-up picture of Fig.3b around the zero α or minimum point.

It is interesting to note that the minimum of the 360Hz ripple is always reached at a close neighborhood of uniform firing. If the imbalance is increased, then a little firing adjustment may help, see the top curve in Fig.3c.

As previously stated, in this analysis we move α and β firing times by an equal but opposite amount. One may question what happens if the two firings are adjusted arbitrarily, rather than synchronously. Although an arbitrary adjustment of the firing is difficult to implement physically, we still show that the results shown in Figs.2 and 3 have not missed the best possible ripple reduction compared with the arbitrary firing. In Fig.4a, we show a scanning of both α and β from -0.69ms to 0.69ms, independently, for the 5% imbalanced system. The z-axis is the logarithmic value of the 360Hz ripple with respect to the DC. The bottom line in the valley corresponds to the firing control of

α=$-\beta$, which implies that the two firing points shift uniformly in the same direction. This is consistent with the results shown before. A possible lower ripple can be found at α=0 and β=0.69ms(see the arrow A in Fig.4a). Another plot for this specific situation in Fig.4b shows that the ripple at this point is still higher than that on the bottom of the valley. In Fig.4c, we show the same plot as Fig.3a for the balanced case, as long as the rectifier is uniformly fired, i.e., α=$-\beta$, the 360Hz ripple does not appear.

2. Transformer phase imbalance

We have also modified equation (2) to accommodate the situation of phase imbalance rather than amplitude imbalance. Suppose we let every other fundamental waveform be shifted by a certain amount of phase. Using the same procedure as that in the last section, the results are shown in Fig.5. In Fig.5a, the rectifier phase back angle is 7.5 degrees. The 6 curves from bottom to top represent the phase imbalance spaced by 3 degrees from 0 to 15 degrees, respectively. This plot can be compared with the one in Fig.2b where only the amplitude imbalance is varied. In Fig.5b, the curves are replotted under the condition of the phase back angle set at 39.9 degrees. This plot can be compared with the one in Fig.3b.

3. Verification

Another program was developed to verify the results given above. Instead of using equation (2), the rectified waveform is simulated for the different transformer amplitude and phase imbalances. A signal processing program was then applied to these waveforms. In Fig.6, for example, we show the simulated rectified waveforms for the 5% amplitude imbalance case, with different phase back angles of 7.5, 18.3, 39.9 degrees, respectively. The spectrum analysis of these waveforms using FFT program gives results that are close to the ones obtained in the last two sections of this report.

III. A Real Example

The real cause of the subharmonic ripple reduction limit for a multiphase rectifier is a comprehensive topic. The results that appear on the output of a rectifier system can however always be represented as a combination of the amplitude and phase imbalances. Therefore, the analysis shown above can be applied. In this section, we show an example.

Subharmonic ripple reduction has been performed by different people on a 150KW, 12 phase power supply located at the building 911 Westinghouse Lab area. All subharmonic ripples but the 360Hz can be reduced down to as low as -68db with respect to the DC level. The 360Hz ripple could only be reduced to about -40db, 25 times higher than the others. To locate the problem, we have measured and analyzed the 60Hz sine waveforms for the two bridges. They are shown in Fig.7, a1 and a2. A slight difference was noticed in the two waveforms. From the waveform spectrums we reproduced the two waveforms using the fundamental, third, fifth, seventh, eleventh, and thirteenth harmonics. The top portions of these two reproduced waveforms are shown in Fig.7b. It is noticed that at the top the imbalance is dominated by amplitude differences, and elsewhere, by phase. In Fig.8a, a pure 60Hz sine waveform is shown by the bold curve superimposed on the others. Both waveforms are distorted. The distortion is however not much. In Fig.8b and 8c, we show the half and the whole cycle waveforms where the difference between the two as observed by eye may be probably treated as trivial at many occasions. After all, the sum of the harmonics from the third to thirteenth for the two waveforms are only 1.8% and 1.5% with respect to the fundamental, respectively. Fig.9a shows the spectrum of one waveform, and 9b shows the harmonics that are superimposed on the 60Hz sine waveform of the two bridges.

The amplitude imbalance at the top is about 2%, while the largest phase difference at the worst place is about 3.5 degrees. If for example, the rectifier phase back angle is 39.9 degrees, i.e., τ_0=5.667ms, then from Fig.7b we may assume the transformer has a

phase imbalance of, say, 3.3 degrees. This single factor alone results in a 360Hz ripple reduction limit of about -47db, as shown in Fig.10. Thus, the 360Hz ripple is very sensitive to very small amounts of phase error.

IV. Conclusion

To conclude, we have the following comments.

1. The 360Hz ripple reduction limit shown in this note may be used to evaluate the real situation found in multiphase power supplies. For instance, if a 12 phase rectifier is found with the power supply input waveform imbalance that is equivalent to 5% amplitude imbalance, and the operating phase back angle is about 40 degrees, then the minimum 360Hz ripple reduction that can be expected by using any firing adjustment is -39db with respect to the DC. This is high. To fix the problem, the only means is to fix the transformer to reduce the amplitude imbalance.

2. The analysis for the 360Hz ripple is believed to be applicable to the other components. For instance, if one SCR is significantly different from the others, then there exists some inherent 60Hz ripple in the rectifier system that cannot be fixed by firing control. Fortunately, the problems caused from these sources are trivial compared with the 360Hz ripple.

3. If the magnitudes of the low frequency subharmonic ripples such as 60Hz, 120Hz and 180Hz are high, then sometimes the 360Hz ripple can be reduced below the limit shown above. The reason is that due to the nonlinearity of the multiphase rectifier system, the low frequency subharmonic ripples may generate 360Hz harmonic that reduces the original 360Hz ripple. Since all the low frequency subharmonic ripples are expected to reduce, this type reduction is of little interest in practice.

Appendix

We need the following formulae:

$$\lim_{t\to\infty} \frac{Sin\,\omega t}{\pi\omega} = \delta(\omega) \tag{A-1}$$

$$\lim_{t\to\infty} \frac{Cos\,\omega t}{\pi\omega} = 0 \tag{A-2}$$

$$e^{\pm j\omega t} = Cos\,\omega t \pm jSin\,\omega t \tag{A-3}$$

$$F(j\omega) = \int_{-\infty}^{\infty} f(t)e^{-j\omega t}\,dt \tag{A-4}$$

where δ denotes the delta function, and $F(j\omega)$ is the Fourier Transform of the function $f(t)$.

We may write

$$f(t) \rightarrow F(j\omega) \tag{A-5}$$

Then we have

$$f(t+\alpha) \rightarrow e^{j\omega\alpha}F(j\omega) \tag{A-6}$$

Let $u(t)$ be the step function. Using (A-1 - A-4), we show

$$u(t)Cos\,\omega_0 t \rightarrow \frac{\pi}{2}[\,\delta(\omega-\omega_0) + \delta(\omega+\omega_0)] + \frac{j\omega}{\omega_0^2-\omega^2} \tag{A-7}$$

In fact, we have

$$\int_{-\infty}^{\infty} u(t)Cos\,\omega_0 t e^{-j\omega t}\,dt = \int_{0}^{\infty} Cos\,\omega_0 t e^{-j\omega t}\,dt$$

$$= \frac{1}{2}\int_0^{\infty}(e^{-j(\omega-\omega_0)t} + e^{-j(\omega+\omega_0)t})dt = \frac{1}{2}[\frac{e^{-j(\omega-\omega_0)t}}{-j(\omega-\omega_0)} + \frac{e^{-j(\omega+\omega_0)t}}{-j(\omega+\omega_0)}]\,|_0^{\infty}$$

$$= \frac{1}{2}\lim_{t\to\infty}[\frac{e^{-j(\omega-\omega_0)t}}{-j(\omega-\omega_0)} + \frac{e^{-j(\omega+\omega_0)t}}{-j(\omega+\omega_0)}] + \frac{1}{2}[\frac{1}{-j(\omega-\omega_0)} + \frac{1}{-j(\omega+\omega_0)}]$$

$$= \frac{1}{2j}\lim_{t\to\infty}(\frac{-Cos(\omega-\omega_0)t}{\omega-\omega_0} - \frac{jSin(\omega-\omega_0)t}{\omega-\omega_0} + \frac{Cos(\omega+\omega_0)t}{\omega+\omega_0} - \frac{jSin(\omega+\omega_0)t}{\omega+\omega_0}) + \frac{j\omega}{\omega_0^2-\omega^2}$$

$$= \frac{\pi}{2j}(0 - j\,\delta(\omega-\omega_0) + 0 - j\,\delta(\omega+\omega_0)) + \frac{j\omega}{\omega_0^2-\omega^2}$$

$$= \frac{\pi}{2}[\,\delta(\omega-\omega_0) + \delta(\omega+\omega_0)] + \frac{j\omega}{\omega_0^2-\omega^2}$$

Similarly, we may have

$$u(t)Sin\,\omega_0 t \rightarrow \frac{\pi}{2j}[\,\delta(\omega-\omega_0)+\delta(\omega+\omega_0)] + \frac{\omega_0}{\omega_0^2-\omega^2} \tag{A-8}$$

Using (A-6,A-7), we have

$$u(t)Cos\,\omega_0(t+\alpha) \rightarrow \int_0^\infty Cos\,\omega_0(t+\alpha)e^{-j\omega t}\,dt$$

$$= \int_0^\infty Cos\,\omega_0 t Cos\,\omega_0\alpha e^{-j\omega t}\,dt - \int_0^\infty Sin\,\omega_0 t Sin\,\omega_0\alpha e^{-j\omega t}\,dt$$

$$= Cos\,\omega_0\alpha(\frac{\pi}{2}[\,\delta(\omega-\omega_0)+\delta(\omega+\omega_0)] + \frac{j\omega}{\omega_0^2-\omega^2}) - Sin\,\omega_0\alpha(\frac{\pi}{2j}[\,\delta(\omega-\omega_0)+\delta(\omega+\omega_0)] + \frac{\omega_0}{\omega_0^2-\omega^2})$$

Noting that the delta functions only contribute to the frequencies $\pm\omega_0$, therefore, if the frequencies are not concerned, we may have

$$u(t)Cos\,\omega_0(t+\alpha) \rightarrow Cos\,\omega_0\alpha\frac{j\omega}{\omega_0^2-\omega^2} - Sin\,\omega_0\alpha\frac{\omega_0}{\omega_0^2-\omega^2} \tag{A-9}$$

Similarly, using (A-6,A-8), we have

$$u(t)Sin\,\omega_0(t+\alpha) \rightarrow Cos\,\omega_0\alpha\frac{\omega_0}{\omega_0^2-\omega^2} + Sin\,\omega_0\alpha\frac{j\omega}{\omega_0^2-\omega^2} \tag{A-10}$$

Now, we consider the time function for the waveform shown in Fig.1.

$$\begin{aligned} f(t) &= [u(t)-u(t-\tau-\alpha-\beta)]Sin\,\omega_0(t+\tau_0-\alpha) \\ &+ k[u(t-\tau-\alpha-\beta)-u(t-2\tau)]Sin\,\omega_0(t+\tau_0-\tau-\alpha) \end{aligned} \tag{A-11}$$

Using (A-6,A-10), the Fourier Transform of $f(t)$ can be written as

$$F(j\omega) = Cos\,\omega_0(\tau_0-\alpha)\frac{\omega_0}{\omega_0^2-\omega^2} + Sin\,\omega_0(\tau_0-\alpha)\frac{j\omega}{\omega_0^2-\omega^2}$$

$$- e^{-j\omega(\tau+\alpha+\beta)}\,[Cos\,\omega_0(\tau+\tau_0+\beta)\frac{\omega_0}{\omega_0^2-\omega^2} + Sin\,\omega_0(\tau+\tau_0+\beta)\frac{j\omega}{\omega_0^2-\omega^2}]$$

$$+ ke^{-j\omega(\tau+\alpha+\beta)}\,[Cos\,\omega_0(\tau_0+\beta)\frac{\omega_0}{\omega_0^2-\omega^2} + Sin\,\omega_0(\tau_0+\beta)\frac{j\omega}{\omega_0^2-\omega^2}]$$

$$- ke^{-j2\omega\tau}\,[Cos\,\omega_0(\tau+\tau_0-\alpha)\frac{\omega_0}{\omega_0^2-\omega^2} + Sin\,\omega_0(\tau+\tau_0-\alpha)\frac{j\omega}{\omega_0^2-\omega^2}]$$

After some manipulations, we have

$$F(j\omega) = \frac{1}{\omega_0^2 - \omega^2}\{\omega_0 Cos\,\omega_0(\tau_0-\alpha) + j\,\omega Sin\,\omega_0(\tau_0-\alpha)$$
$$- \omega_0 Cos\,\omega(\tau+\alpha+\beta) Cos\,\omega_0(\tau+\tau_0+\beta) + j\,\omega_0 Sin\,\omega(\tau+\alpha+\beta) Cos\,\omega_0(\tau+\tau_0+\beta)$$
$$- j\,\omega Cos\,\omega(\tau+\alpha+\beta) Sin\,\omega_0(\tau+\tau_0+\beta) - \omega Sin\,\omega(\tau+\alpha+\beta) Sin\,\omega_0(\tau+\tau_0+\beta)$$
$$+ k(\omega_0 Cos\,\omega(\tau+\alpha+\beta) Cos\,\omega_0(\tau_0+\beta) - j\,\omega_0 Sin\,\omega(\tau+\alpha+\beta) Cos\,\omega_0(\tau_0+\beta))$$
$$+ k(j\,\omega Cos\,\omega(\tau+\alpha+\beta) Sin\,\omega_0(\tau_0+\beta) + \omega Sin\,\omega(\tau+\alpha+\beta) Sin\,\omega_0(\tau_0+\beta))$$
$$+ k(-\omega_0 Cos\,2\omega\tau Cos\,\omega_0(\tau+\tau_0-\alpha) + j\,\omega_0 Sin\,2\omega\tau Cos\,\omega_0(\tau+\tau_0-\alpha))$$
$$+ k(-j\,\omega Cos\,2\omega\tau Sin\,\omega_0(\tau+\tau_0-\alpha) - \omega Sin\,2\omega\tau Sin\,\omega_0(\tau+\tau_0-\alpha))\} \qquad \text{(A-12)}$$

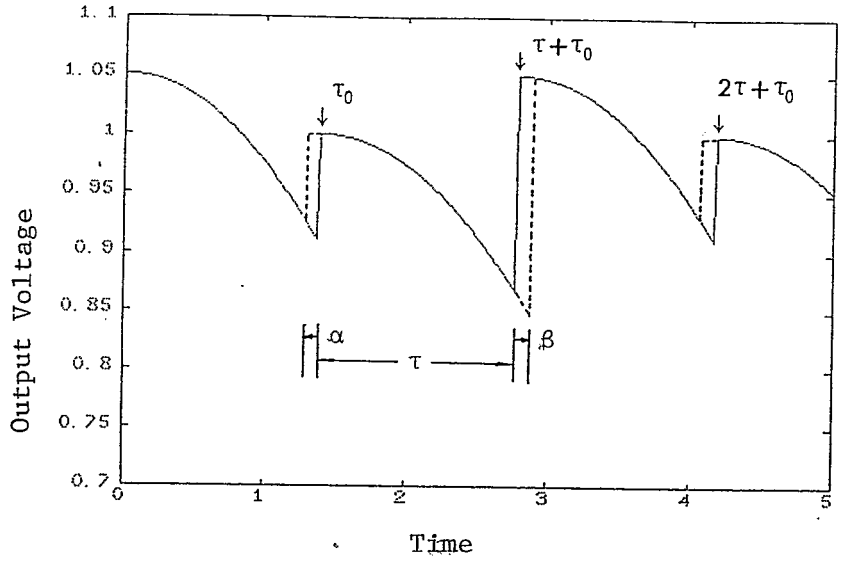

Fig.1

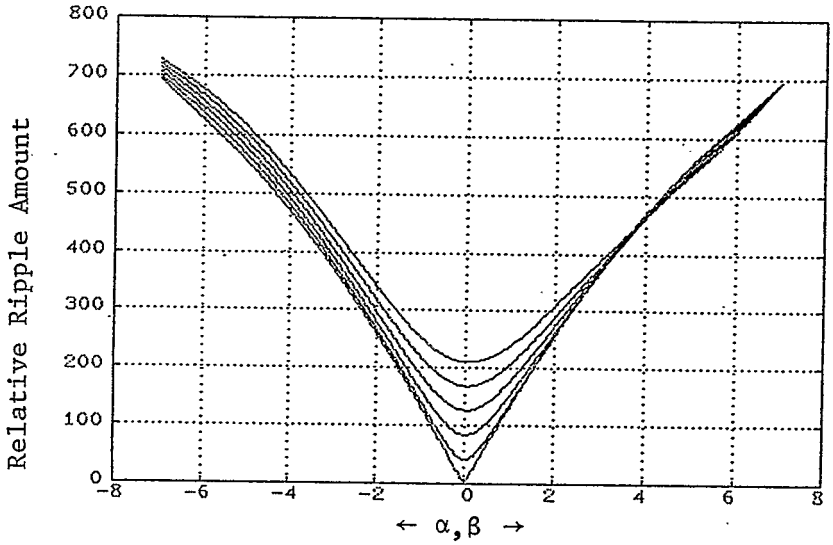

Top to Bottom Curves

ϵ=0.05
0.04
0.03
0.02
0.01
0.00

Fig.2a

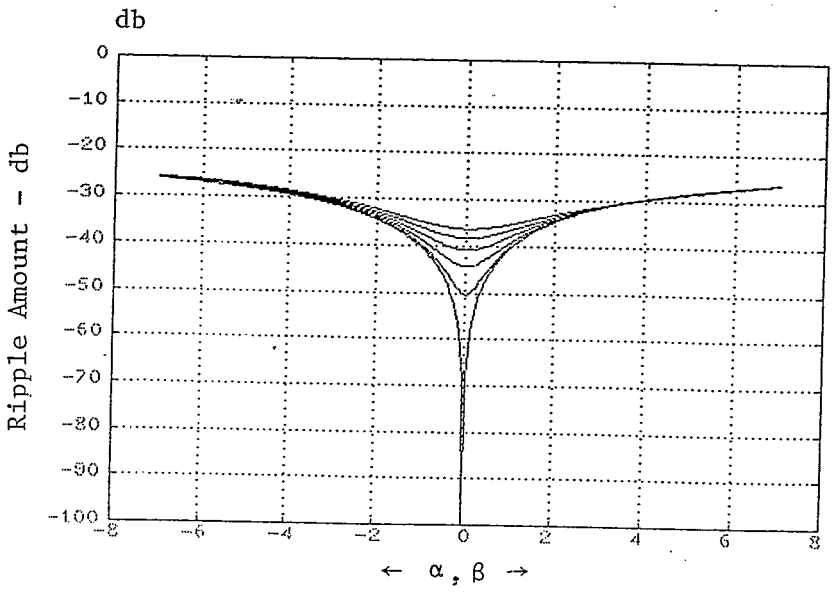

Top to Bottom Curves

ϵ=0.05
0.04
0.03
0.02
0.01
0.00

Fig.2b

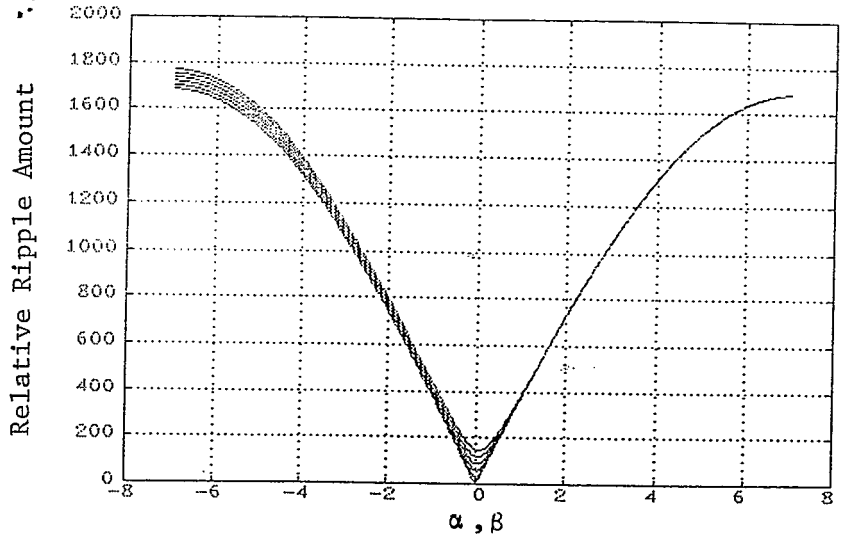

Fig.3a

0.1ms

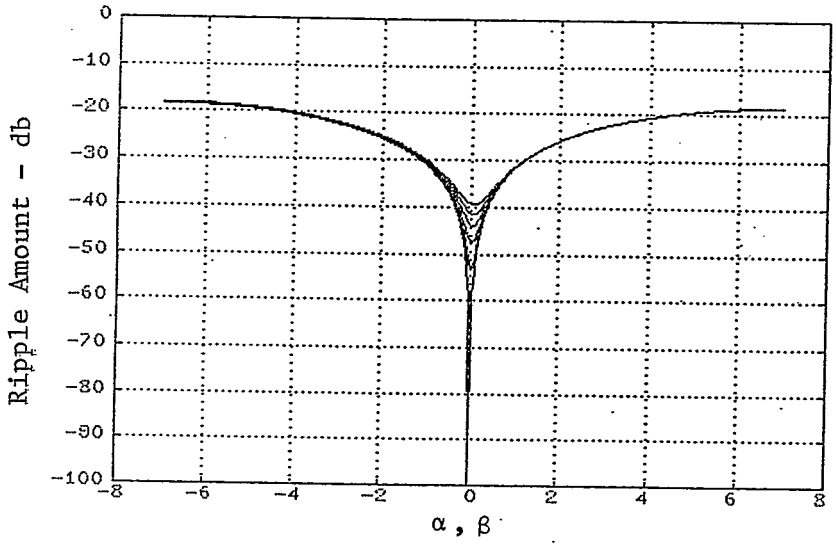

Top to Bottom Curves

ϵ=0.05
0.04
0.03
0.02
0.01
0.00

Fig.3b

0.1ms

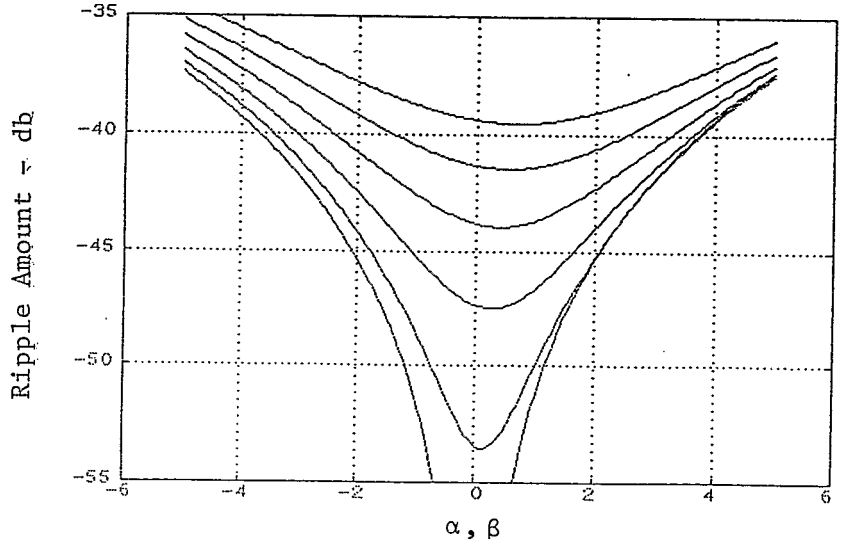

Fig.3c

0.1ms

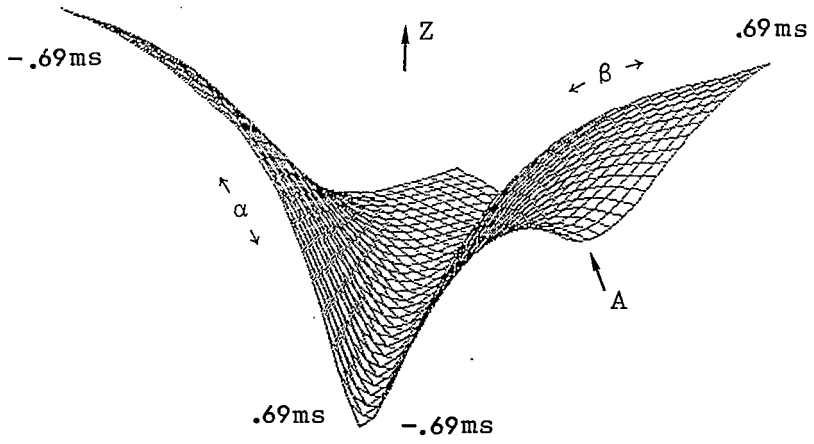

Fig.4a

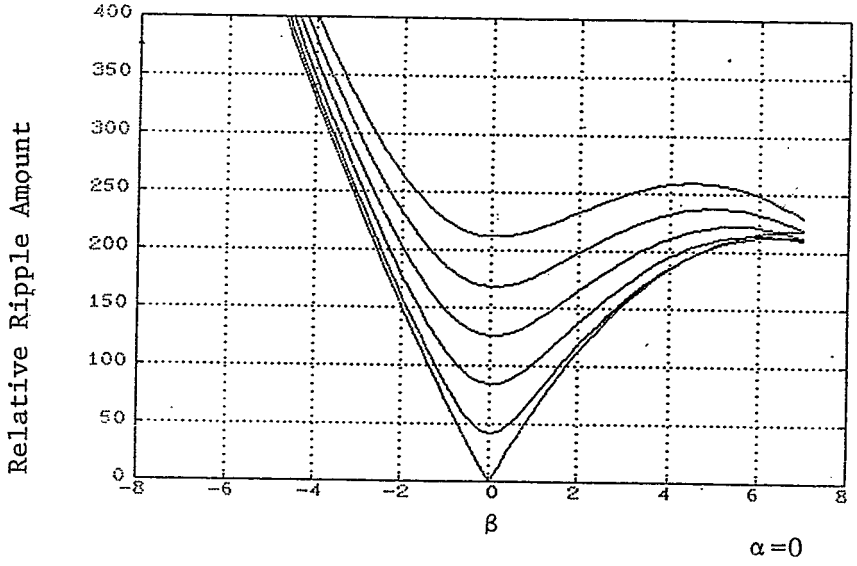

Top to Bottom Curves

ϵ=0.05
0.04
0.03
0.02
0.01
0.00

Fig.4b

0.1ms

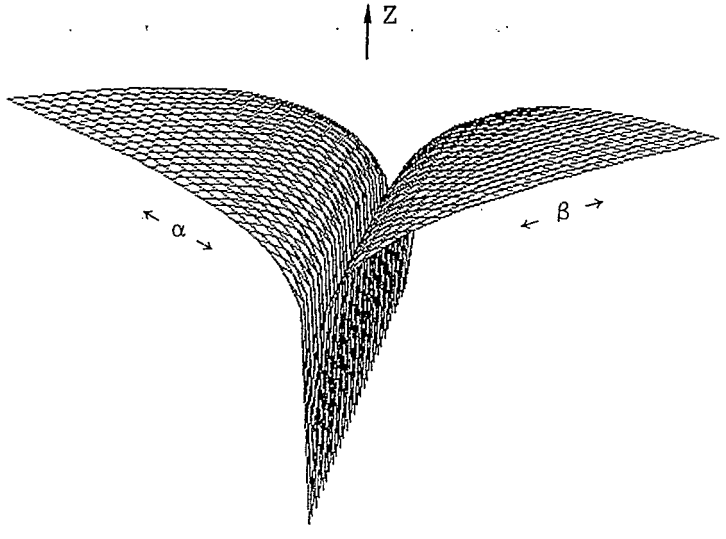

Fig.4c

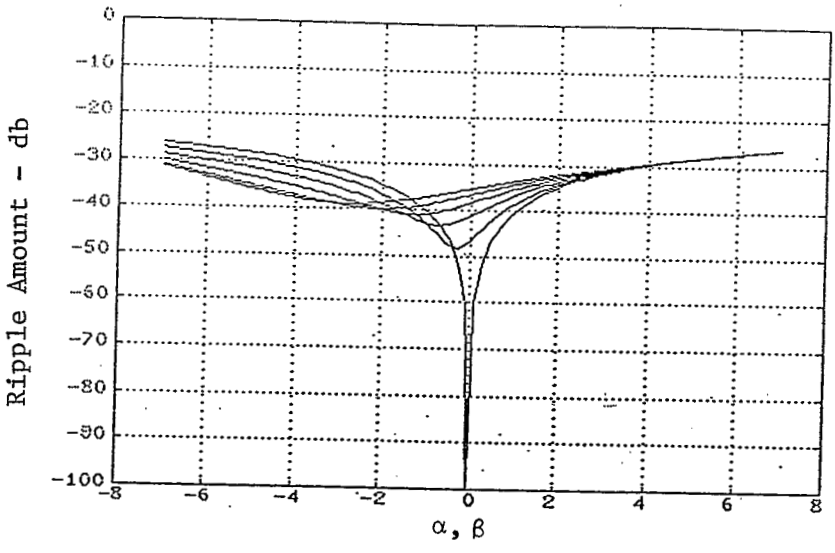

Fig.5a

0.1ms

Top to Bottom Curves

$\Delta\Phi$ =15°
12°
9°
6°
3°
0°

Phase Back Angle = 7.5°

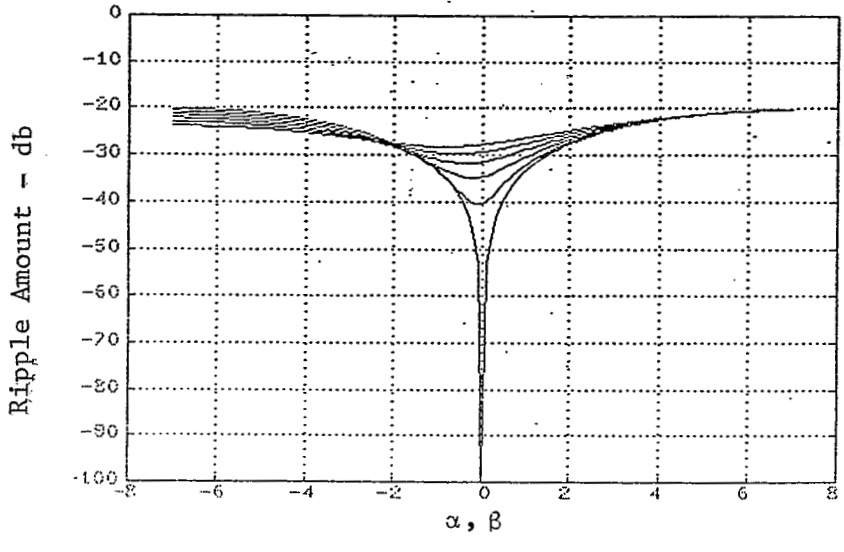

Fig.5b

0.1ms

Phase Back Angle = 39.9°

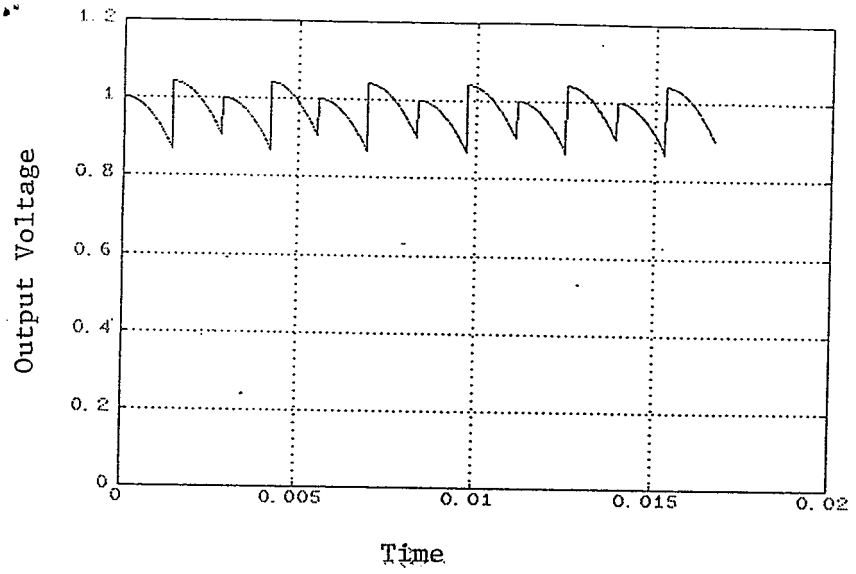

Fig.6a

Phase Back Angle = 7.5°

sec.

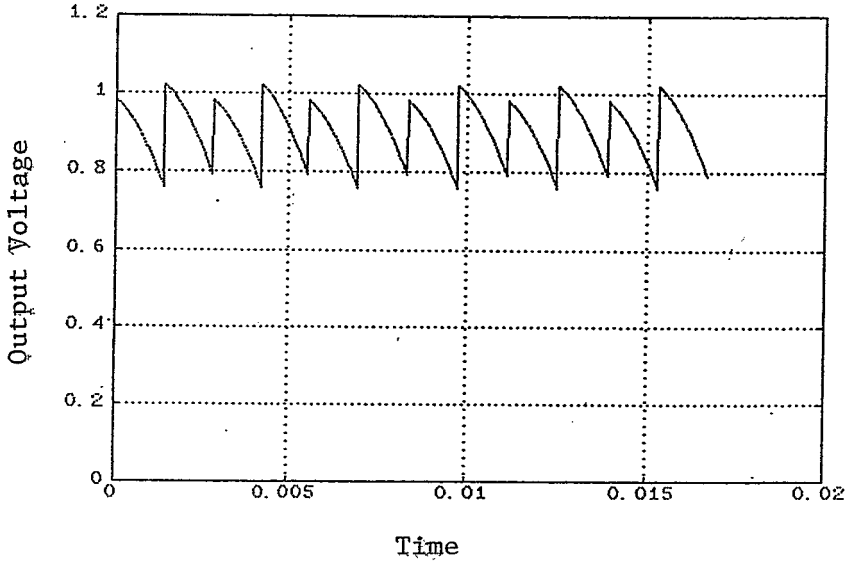

Fig.6b

Phase Back Angle = 18.3°

sec.

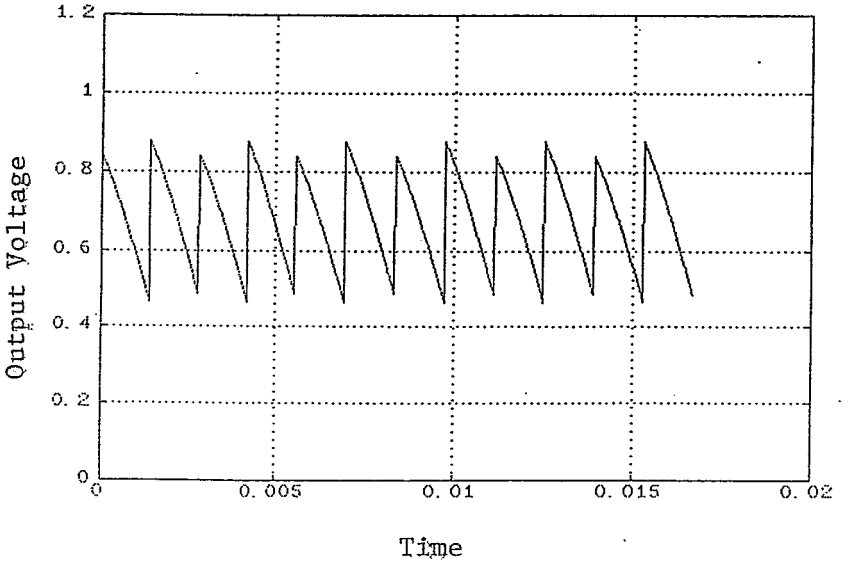

Fig.6c

Phase Back Angle = 39.9°

sec.

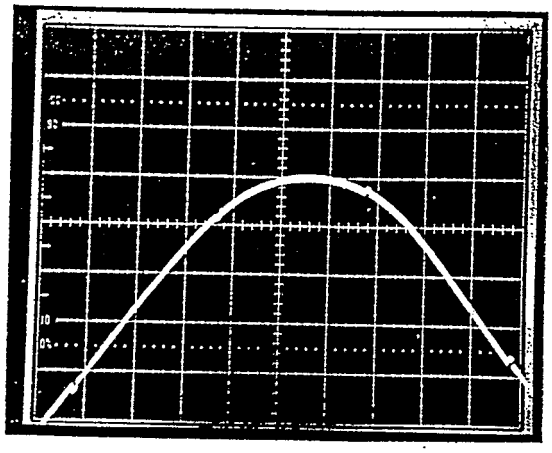

Fig.7a1

Two Bridge Waveforms

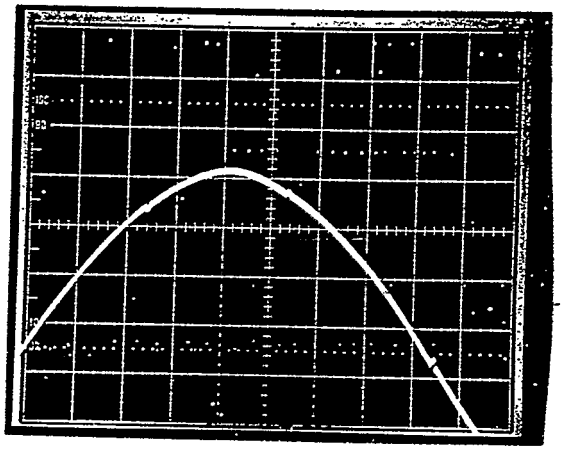

Fig.7a2

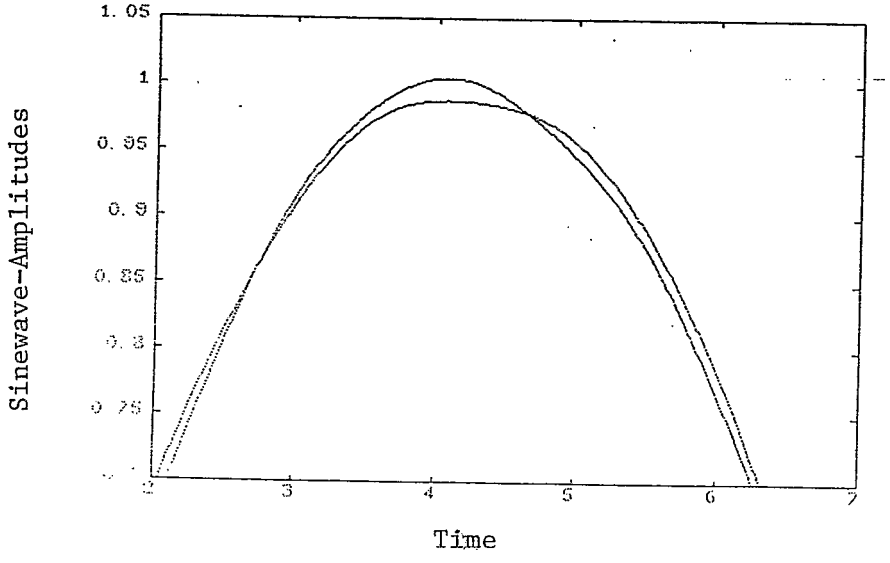

Fig.7b

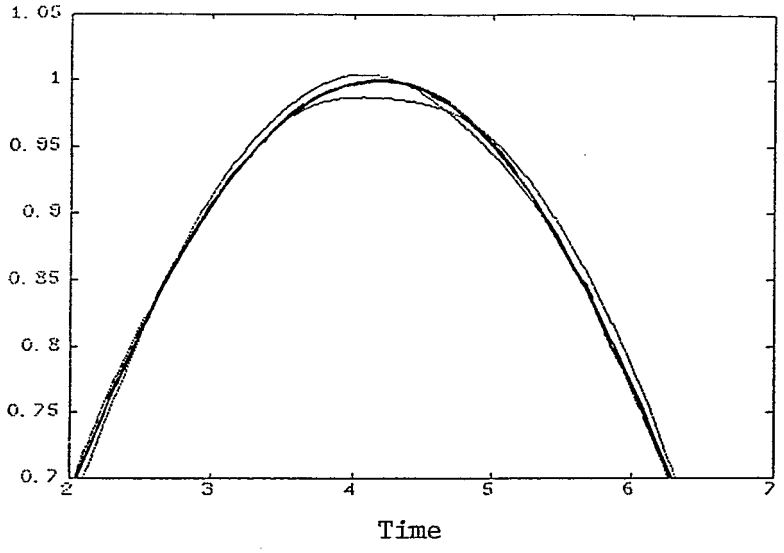

Fig.8a

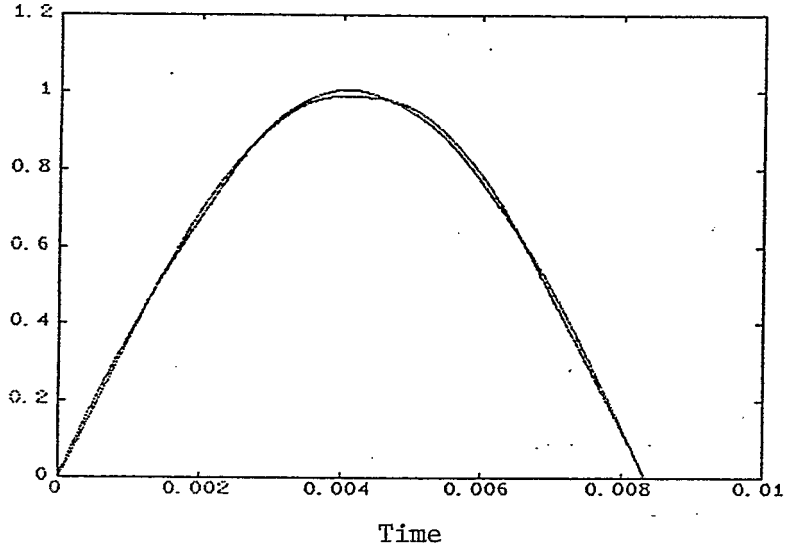

Fig.8b

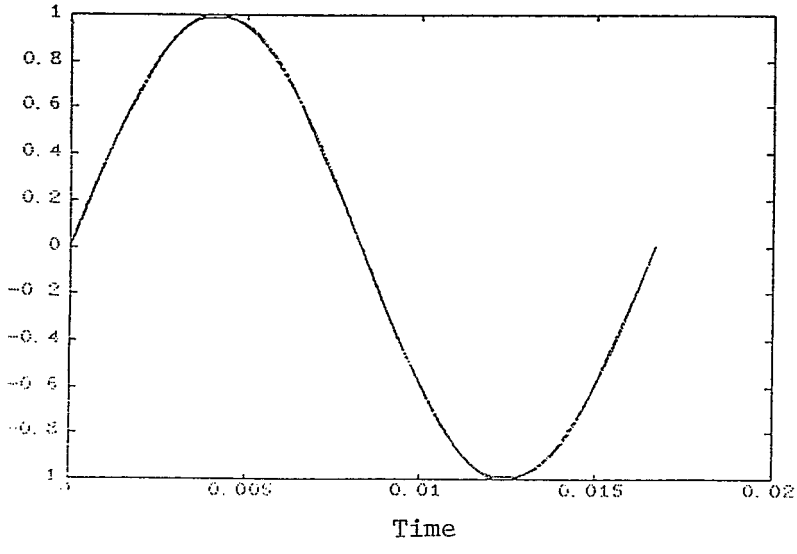

Fig.8c

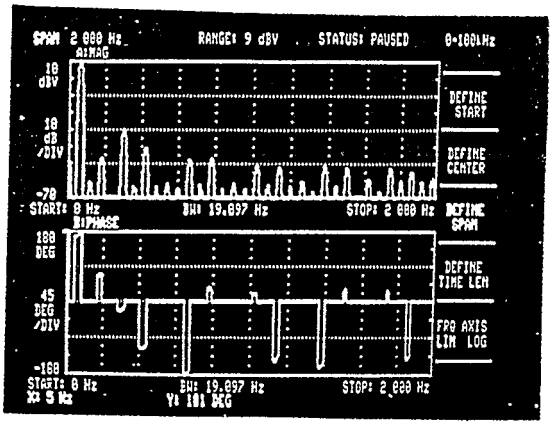

Fig.9a

Bridge A, Spectrum

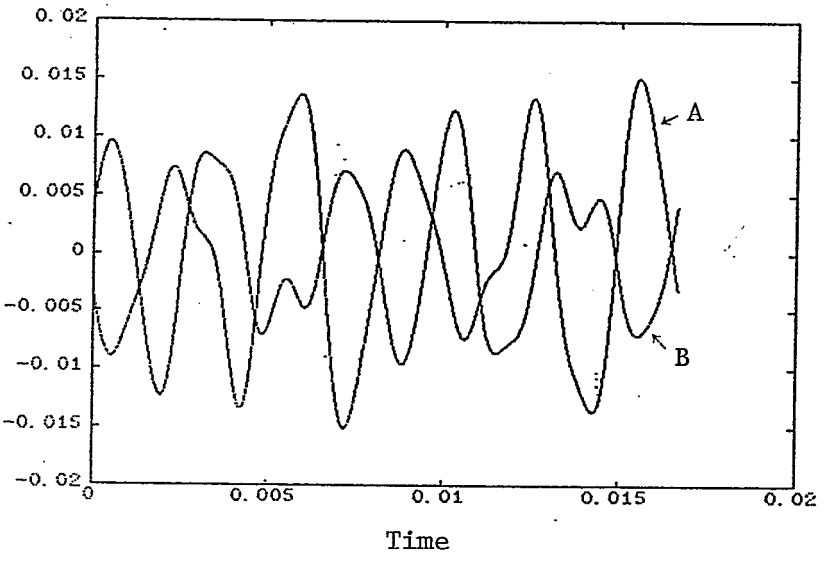

Fig.9b

A: Bridge A

B: Bridge B

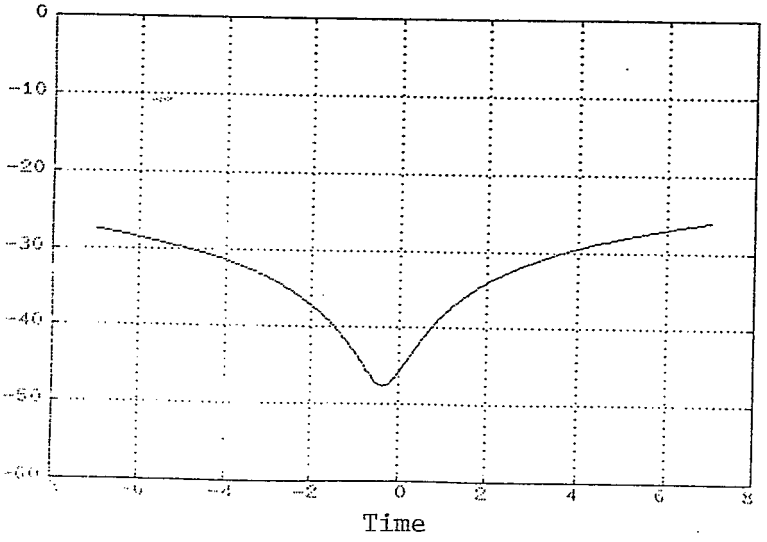

Fig.10

0.1ms